Evidence for crucial electrostatic interactions between Bcl-2 homology domains BH3 and BH4 in the anti-apoptotic Nr-13 protein

Philippe LALLE*[1], Abdel AOUACHERIA*[1], Agnès DUMONT-MISCOPEIN*[1], Martin JAMBON*[2], Séverine VENET*[1], Hélène BOBICHON†, Pierre COLAS‡, Gilbert DELÉAGE*[2], Christophe GEOURJON*[2] and Germain GILLET*[1,3]

*Institut de Biologie et Chimie des Protéines, UMR 5086 CNRS/Université Claude Bernard Lyon 1, 7 passage du Vercors, 69367 Lyon Cedex 07, France, †Unité Median, CNRS FRE 2141, UFR de Pharmacie, 1 rue du Maréchal Juin, 51095 Reims Cedex, France, and ‡Laboratoire de Biologie Moléculaire et Cellulaire, UMR 5665 CNRS/ENS, Ecole Normale Supérieure de Lyon, 46 allée d'Italie, 69364 Lyon Cedex 07, France

Nr-13 is an anti-apoptotic member of the Bcl-2 family previously shown to interact with Bax. The biological significance of this interaction was explored both in yeast and vertebrate cells and revealed that Nr-13 is able to counteract the pro-apoptotic activity of Bax. The Bax-interacting domain has been identified and corresponds to α-helices 5 and 6 in Nr-13. Site-directed mutagenesis has revealed that the N-terminal region of Nr-13 is essential for activity and corresponds to a genuine Bcl-2 homology domain (BH4). The modelling of Nr-13, based on its similarity with other Bcl-2 family proteins and energy minimization, suggests the possibility of electrostatic interactions between the two N-terminal-conserved domains BH4 and BH3. Disruption of these interactions severely affects Nr-13 anti-apoptotic activity. Together our results suggest that electrostatic interactions between BH4 and BH3 domains play a role in the control of activity of Nr-13 and a subset of Bcl-2 family members.

Key words: apoptosis, Bcl-2, Nr-13.

INTRODUCTION

Cellular self-destruction by apoptosis is a biological phenomenon of major importance. In multicellular organisms, the balance between apoptosis and cell proliferation controls tissue homoeostasis. Deregulation of apoptosis may lead to degenerative disorders, tumour formation or auto-immune diseases (reviewed in [1]).

One of the main features of apoptosis is the irreversible activation of a cascade of proteases (caspases), which leads to the hydrolysis of numerous intracellular proteins and eventually cell death. Members of the Bcl-2 family of proteins are key regulators of the apoptotic pathway. Some are activators of apoptosis, whereas others are anti-apoptotic (reviewed in [2]). Pro-apoptotic proteins Bax or Bak are required to initiate most forms of apoptosis [3]. Multiple interactions between pro- and anti-apoptotic proteins have been described, e.g. between Bax and apoptosis inhibitors Bcl-2 [4], Bcl-xL [5] or A1/BFL-1 [6], and recently between Bax and Bak [7]. This network of interactions controls cellular response to apoptotic stimuli [8]. Currently three (non-exclusive) models are used to explain Bcl-2 function. These models describe Bcl-2 proteins as (i) ion channels, (ii) modulators of caspase activation, or (iii) inhibitors of cytochrome c export from mitochondria (reviewed in [9]). These proteins show four homology domains (BH1–BH4) forming α-helices. Among at least 16 Bcl-2 homologues found in humans to date, only four structures have been experimentally resolved (Bcl-xL, Bcl-2, Bid and Bax). Although these proteins play very different roles in apoptosis, their overall folding is similar. The three-dimensional (3D) structure of Bcl-xL shows that the BH1–BH3 domains belong to a region of the protein which is thought to interact with the lipid bilayer, forming pores in the outer mitochondrial membrane as the colicins do in bacterial membranes [10,11]. The BH4 domain, located in the N-terminal

moiety, contains an amphipathic helix that probably faces the cytosol. This domain is linked up to the rest of the protein by a flexible loop of undefined structure, which is involved in regulation of anti-apoptotic activity [2,12], although it has also been shown to be dispensable for Bcl-xL antiapoptotic activity [10]. Differences in mobility of this loop have been observed between Bid, Bax and Bcl-xL, which share high structure similarity [10,13,14]. Deletion of the BH4 domain results in a total inactivation of Bcl-2 or Bcl-xL [15]. Mutagenesis experiments suggest that hydrophobic interactions between BH4 and surrounding domains participate in the appropriate folding of these proteins [15–17].

In contrast to the C-terminal moiety, the N-terminal moiety (BH4 plus loop) is poorly conserved among Bcl-2 family members [2]. This suggests that their C-terminal halves share the same colicin-like structure, while the BH4 region could confer specificity on each individual member of the family, possibly through interaction with specific partners. A number of ligands have been reported to interact with BH4, among them CED-4 [15], VDAC [18], and calcineurin [19]. Although the precise biological significance of these different interactions remains to be elucidated, these data have clearly identified BH4 as an important functional domain of the Bcl-2 family of apoptosis inhibitors.

Nr-13 belongs to this family, and was first characterized in avian retina cells transformed by the Rous sarcoma virus [20]. Activation of Nr-13 expression may be an important step in neoplastic transformation induced by the tyrosine kinase p60^{v-src} [21,22]. Nr-13 has been reported to associate with Bax, suggesting that it might counteract its cytotoxic effect [23]. Very recently we have shown that Nr-13 is able to interact with cytochrome c, but its mechanism of action remains underexplored [24]. A precise characterisation of Nr-13 functional domains may shed light on some important features of cell transformation by p60^{v-src} and related kinases. In this paper, we present the results of a

---

structure–function analysis of Nr-13 based on site-directed mutagenesis of its N-terminal region and computer-assisted modelling. Our results elucidated a new regulatory mechanism controlling the activity of Nr-13 and related inhibitors of apoptosis.

MATERIALS AND METHODS

Molecular modelling

The chicken Nr-13 (GenBank accession number: AF375661) and human Bcl-xL (SWISSPROT code: BCLX_HUMAN) sequences were automatically aligned using CLUSTALW 1.8 [25], the predicted and observed secondary structures of Nr-13 and Bcl-xL were compared, and the alignment of the N-terminal region of both sequences was manually optimised accordingly. The resulting alignment was used to define the template regions of Bcl-xL usable for the modelling. Molecular modelling was performed using Geno3D software [26]. Briefly, the known 3D structure of Bcl-xL (protein data bank code: 1MAZ) was used to calculate interatomic distances and dihedral angles. Ten 3D structures were generated from these sets of constraints by using a distance geometry protocol (similar to that used in NMR), with the default parameters sets of the X-PLOR 3.85 software program [27]. Each structure was regularized by simulated annealing (2000 steps) and energy minimization (2000 steps). The quality of the models was assessed with the PROCHECK tools [28]. The model exploited was that with the lowest energy. All protein sequence analyses were carried out at the NPS@Web server (http://npsa-pbil.ibcp.fr).

Plasmid constructions for transient transfections in Rat-1 cells

Chicken *nr-13* cDNA, cloned into the polylinker region of pBSK (pBSK-Nr-13), was PCR-amplified with appropriate primers (Table 1). PCR products were *Not*I digested and subcloned in pcDNA3.1/His C (Life Technologies, Cergy Pontoise, France). The correct orientation was verified by *Hin*dIII/*Afl*II digestion. For point mutants, a two-step PCR strategy was used. pBSK-

Table 1   Primers used to generate Nr-13 mutations

Deletion mutants in yeast	Sequence of forward and reverse primer pairs
1–52	5′-ATATGAATTCATGCCGGGCTCTCTGAAGG-3′ 5′-ATATCTCGAGGGGATCGGAAGAAGGGCCGCTC-3′
1–63	5′-ATATGAATTCATGCCGGGCTCTCTGAAGG-3′ 5′-ATATCTCGAGCTCCCGCGGCTCGGCCCGCGC-3′
58–157	5′-ATATGAATTCCGGGGCCGAGCCGCGGGAGGCG-3′ 5′-ATATCTCGAGATTGCTTAAGGTACTGTTCTGG-3′
1–157 (ΔTM)	5′-ATATGAATTCATGCCGGGCTCTCTGAAGG-3′ 5′-ATATCTCGAGATTGCTTAAGGTACTGTTCTGG-3′
Point mutants generated in pcDNA3.1 vector	
D15A	5′-TGCTGCTGGAGGCTTACTTCCAGCA-3′ 5′-TGCTGGAAGTAAGCCTCCAGCAGCA-3′
R36A	5′-GCGGCCGAGCTGGCGCGGGCGGCGGCCGAG-3′ 5′-CTCGGCCGCCGCCCGCGCCAGCTCGGCCGC-3′
R20A	5′-GAGGACTACTTCCAGCACGCCGCCGGCGGCGCCGCGCTG-3′ 5′-CAGCGCGGCGCCGCCGGCGGCGTGCTGGAAGTAGTCCTC-3′
E43A	5′-GCGGCCGAGCTGGCGCGCGCCGAGAGCGG-3′ 5′-CCGCTCTCGGCGCGCGCCAGCTCGGCCGC-3′
D15A-R20A	5′-TGCTGCTGGAGGCTTACTTCCAGCACGCGGCCGGCGGGGGC-3′ 5′-GCCCCGCCGGCCGCGTGCTGGAAGTAAGCCTCCAGCAGCA-3′
External primers	5′-ATGCGGCCGCTAATGCCGGGGCTCTCTG-3′ 5′-ATGCGGCCGCCTACCGCACCACCAAGAG-3′

Nr-13 was used as a template for the first step to generate, in parallel, two overlapping fragments. One fragment was amplified with the forward external primer and the reverse primer specific to the mutation, while the other was amplified with the forward specific primer and the reverse external primer. After purification, the two PCR products were mixed and used as template for the second-step PCR using the two external primers. The full-length mutant PCR products were then *Not*I digested and subcloned into pcDNA3.1/His (Invitrogen). The correct orientation was checked by *Hin*dIII/*Afl*II digestion. Both truncations and point mutations were checked by complete sequencing of the insert. pBS-KS containing the full length murine *bcl-2* cDNA (a gift from Dr S. J. Korsmeyer, Dana-Farber Cancer Institute, Boston, MA, U.S.A.) was *Hin*dIII/*Eco*RI digested and the insert was subcloned into RcCMV (Life Technologies) to generate the RcCMV-Bcl-2 expression vector. RcCMV-Bax [with a cyto-megalovirus (CMV) promoter and a haemagglutinin (HA) tag upstream of the mouse *bax* open reading frame (ORF) cDNA] and RcCMV-luciferase were gifts from Dr S. J. Korsmeyer.

Coupled transcription/translation

Production of wild-type (wt) Nr-13 and its mutants, from the pcDNA3.1/His C constructs, was checked using a commercially available coupled transcription/translation system (TNT® T7 Coupled Reticulocyte Lysate System; Promega, Charbonnières, France). Empty pcDNA3.1/His C vector was incorporated into the same series as a control. Experiments were performed according to manufacturer's recommendations in the presence of 1 μg of each vector. Samples were separated by SDS/PAGE (15 % gel) and exposed overnight with a BIOMAX™ MR autoradiography film (Eastman Kodak Company, Rochester, NY, U.S.A.).

Plasmid constructions for two-hybrid experiments and growth assays in yeast

Interaction mating assays were performed mostly as described previously [29] using EGY48 and EGY42 strains [30]. EGY42 was co-transformed with pSH18-34 bearing eight LexA operators upstream a *LacZ* reporter gene, and pEG202 or pGILDA directing the expression of various LexA fusion proteins. pEG202 contained a 2 μm replication origin and a constitutive ADH1 promoter, while pGILDA harbours a CEN/ARS replication origin and a GAL1 promoter. EGY48 was transformed with pJG4-5 directing the expression of various fusion proteins (B42 activation domain fused with Bcl-2 family member cDNAs) under the GAL1 promoter. All vectors have been described previously [31].

We generated Nr-13 truncations by PCR using primers shown in Table 1 and pBSK-Nr-13 wt or mutant as a template. Fragments were digested by *Eco*RI and *Xho*I and inserted into pGILDA or pJG4-5. pJG4-5-Bcl-xL (human), pJG4-5-Bcl-xS (human), pJG4-5-Bcl2(72-218) (human) and pJG4-5-Bax ΔTM (murine) have been described previously [32,33]. A LexA-Bax ΔTM vector (obtained from Dr J. C. Reed, The Burnham Institute, La Jolla, CA, U.S.A.) was digested with *Eco*RI and *Xho*I and ligated into *Eco*RI/*Xho*I-cut pGILDA to generate pGILDA-Bax ΔTM. pGILDA-Bax was obtained after RcCMV-Bax PCR amplification. The amplified product was digested with *Eco*RI and *Xho*I and ligated into *Eco*RI/*Xho*I cut pGILDA. All Bax truncation mutants were generated by PCR amplification using pJG4-5-Bax ΔTM as a template (primer sequences available upon request) and subcloned into *Eco*RI/*Xho*I-cut pJG4-5. Mouse *bad* ORF cDNA in pSFFV-neo expression vector (a gift from Dr S. J. Korsmeyer) was PCR amplified. After *Eco*RI/*Xho*I

digestion the amplified product was ligated into *Eco*RI/*Xho*I-cut pEG202. Sequences corresponding to the putative transmembrane domains of Nr-13, Bcl-2, Bcl-xS, Bcl-xL and Bax were systematically omitted and a stop codon was inserted to avoid problems with targeting of proteins to the nucleus.

Yeast-growth assays

Yeast transformations were performed using the lithium acetate method and transformants were selected and maintained on standard synthetic media [34]. The EGY48 strain was co-transformed with pGILDA-Bax and pJG4-5 encoding wt or point-mutated Nr-13 or Nr-13-ΔTM. Selective media containing 2% glucose was inoculated with a single colony from positive transformants and incubated overnight at 30 °C. Subsequently, cells were washed three times with water. Typically, 10 ml of selective medium with 2% galactose was inoculated at $D_{600} = 0.1$. Growth was monitored for 48 h. Samples were taken at different time points, and cell density was measured by determining the D_{600}. Appropriate dilutions were performed regularly to maintain cells in the exponential growth phase.

Luciferase assays

Rat-1 cells were grown in Dulbecco's modified Eagle's medium (DMEM) with 10% fetal calf serum. The day before transfection, cells were seeded at a density of 8×10^4 in each well of the 12-well dishes. Transfections were performed 18 h after seeding. For each well 75 ng of RcCMV-luciferase expression vector were used and variable amounts of Bax, Bcl-2 or Nr-13 expression vector. In each experiment the total amount of CMV promoter was adjusted in all wells using RcCMV vector; total amount of DNA was then adjusted in all wells using pUC18 vector. The cells were incubated for 4 h in serum-free medium (OPTI-MEM) containing DNA and 3 µl of the cationic lipid LipofectAMINE according to the manufacturer's protocol (Life Technologies). Then an equal volume of DMEM containing 10% serum was added, without removing the transfection mixture, and cells were further incubated for 18 h. Cell viability was estimated by luciferase-assay system according to manufacturer's protocol (Promega). Briefly, cells were washed twice with 1 ml of PBS, incubated for 15 min in 200 µl of reporter-lysis buffer then recovered. Cells (40 µl) were mixed with 200 µl of luciferase-assay reagent. Quantification was performed with a Dynex Technologies luminometer (Chantilly, VA, U.S.A.).

Western-blot analysis

Expression of Bax, Bcl-2 and Nr-13 in Rat-1 cells was checked simultaneously with the luciferase experiments using the highest ratio of each RcCMV vector used for these experiments (200 ng/8×10^4 cells seeded). After separation by SDS/PAGE, Western blots were performed using standard protocols. Bax and Bcl-2 were detected using HA (Y-11) and Bcl-2 (C-2) antibodies, respectively (Santa Cruz Biotechnologies Inc., Heidelberg, Germany) and Nr-13 with the previously described anti-Nr-13 polyclonal antibody [21]. For yeasts, overnight cultures were adjusted to the same D_{600} and the same volume of each culture was used to extract the yeast proteins with lyticase (1 mg/ml) for 1 h at 30 °C. Recombinant B42-Nr-13 proteins and the fusion LexA proteins were detected using antibodies against the B42 activating domain or the LexA protein [polyclonal B42 (FL) sc-8335 and monoclonal LexA (2-12) sc-7544; Santa Cruz Biotechnology].

CD spectra

CD spectra were recorded on a Jobin–Yvon CD6 spectrometer calibrated with ammonium D-10-camphorsulphonate. Calculations were performed with the CD6 software. Assuming the peptide molar ellipticity at 222 nm is exclusively due to α-helix, the helical content was estimated according to the method of Chen et al. [35].

Immunohistochemistry

pcDNA3.1/His C containing either wt Nr-13 or point mutant Nr-13 was PCR amplified with primers 5′-ATATCTCGAGGA-ATGCCGGGCTCTCTGAAGGA-3′ and 5′-TATAGAATTC-CTACCGCACCAAGAGAA-3′. PCR products were *Xho*I/*Eco*RI digested and subcloned into pEGFP-C1, which contained the enhanced green fluorescent protein (EGFP) marker gene (ClonTech Laboratories, Erembodegem, Belgium). Transfections were performed on COS-7 (African-green-monkey fibroblasts) or QM7 (Japanese-quail-muscle clone 7) cells. Briefly, 2.5×10^4 cells were seeded on 8-well culture chambers (BD Falcon, Becton Dickinson, Franklin Lakes, NJ, U.S.A.) and grown for 24 h at 37 °C before transfection with the appropriate pEGFP-C1 recombinant vector using Fugene 6 reagent (Roche Diagnostics, Meylan, France) following the manufacturer's instructions and as described previously [36]. To visualize mitochondria after 24 h, cells were loaded with MitoTracker™ (MitoTracker™ Red CMXRos, Molecular Probes Europe BV, Leiden, The Netherlands) by incubating in the same medium containing 250 nM MitoTracker™ (freshly prepared in DMSO) for 15 min at 37 °C. Care was taken to ensure minimum exposure of cultures to light in all subsequent manipulations. After three washes with PBS, cells were fixed with 4% paraformaldehyde in PBS for 20 min at 4 °C and incubated for 30 min with 1 µg/ml Hoechst 33258 in PBS to visualize nuclei. Representative fields of cells were photographed under fluorescence microscopy (Zeiss microscope) to visualize green fluorescent protein (GFP), bisbenzimide and MitoTracker™ staining (Kodak film, ASA 200).

RESULTS

Nr-13 inhibits Bax-induced apoptosis

Analysis of Nr-13 secondary structure and multiple sequence alignments showed that Nr-13 possessed the typical organization
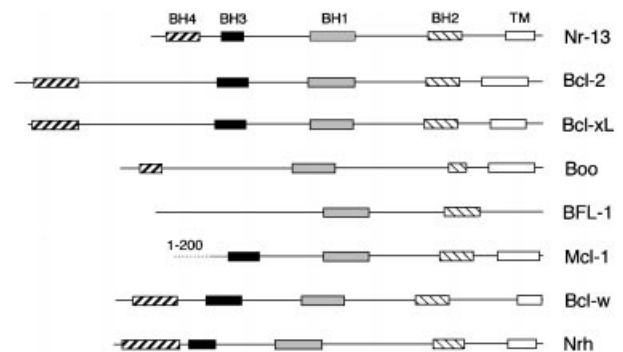

Figure 1   Comparison of domain organization of several Bcl-2 family anti-apoptotic members

All proteins are from human except Nr-13 (chicken) and Boo (mouse). BH1 to BH4 are conserved sequence motifs. TM represents the hydrophobic region thought to act as a membrane anchor. Nrh is a recently described Nr-13 human homologue [36,48–50].
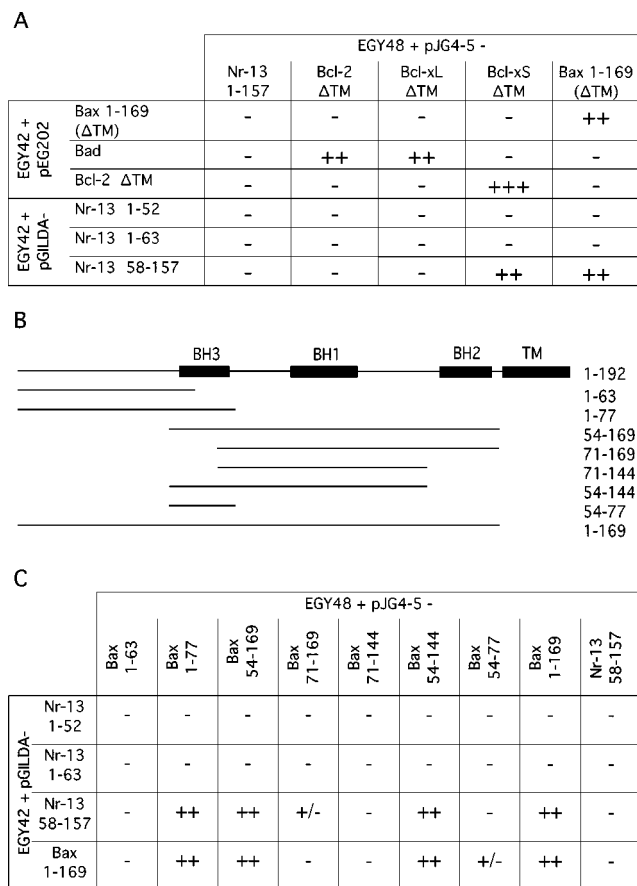
A

	EGY48 + pJG4-5 -				
	Nr-13 1-157	Bcl-2 ΔTM	Bcl-xL ΔTM	Bcl-xS ΔTM	Bax 1-169 (ΔTM)
EGY42 + pEG202 Bax 1-169 (ΔTM)	-	-	-	-	++
Bad	-	++	++	-	-
Bcl-2 ΔTM	-	-	-	+++	-
EGY42 + pGILDA- Nr-13 1-52	-	-	-	-	-
Nr-13 1-63	-	-	-	-	-
Nr-13 58-157	-	-	-	++	++

B

C

	EGY48 + pJG4-5 -								
	Bax 1-63	Bax 1-77	Bax 54-169	Bax 71-169	Bax 71-144	Bax 54-144	Bax 54-77	Bax 1-169	Nr-13 58-157
EGY42 + pGILDA- Nr-13 1-52	-	-	-	-	-	-	-	-	-
Nr-13 1-63	-	-	-	-	-	-	-	-	-
Nr-13 58-157	-	++	++	+/-	-	++	-	++	-
Bax 1-169	-	++	++	-	-	++	+/-	++	-

Figure 2   Nr-13 interacts with Bax through BH1 and BH2

(**A**) Interaction-trap assay using fusion protein LexA-Nr-13 as a bait. Nr-13 deletion mutants 1–52 and 1–63 (both containing BH4 and BH3 domains, see Figure 1A), were unable to interact with activation domain fusion proteins Bax and Bcl-xS in contrast with deletion mutant 58–157 (BH1 and BH2 only). (**B**) Map of Bax deletion mutants. (**C**) Two-hybrid analysis of Nr-13 and Bax using deletion mutants of each protein.

Figure 3   Nr-13 inhibits Bax cytotoxicity in yeast and vertebrate cells

(**A**) Growth curves of yeast strains expressing Bax and the proteins to be tested. After overnight growth in the presence of glucose, EGY48 yeast cells were cultured in the presence of 2% galactose to induce them to express Bax only, or Bax with Bcl-2 ΔTM, Nr-13 or Nr-13 ΔTM. Growth was monitored by measurement of D_{600}. (**B**) Measurement of luciferase activity was used as an indicator of viability in Rat-1 cells. Cells were transfected and expression of the corresponding proteins was confirmed. The insets show representative Western blots; each panel shows untransfected cells (left-hand lane) and transfected cells (right-hand lane). Luciferase activity was measured 18 h after transfection as described in the Experimental procedures. Expression of Bax results in massive cell death (lane 2), which is reduced by Nr-13 (lanes 3–8) and Bcl-2 (lanes 9–14). Results are presented as means ± S.D. of three experiments.

of Bcl-2 family proteins, with seven α-helices and three Bcl-2 homology domains: BH1–BH3 (Figure 1). The first α-helix corresponded to a fourth homology domain (BH4) present in Bcl-2, Bcl-xL and a number of anti-apoptotic proteins. However, this region of Nr-13 shared little similarity with other BH4 domains, suggesting that it diverged more rapidly during evolution. This situation raised the possibility that, although it is a potent cell-death inhibitor, Nr-13 might be devoid of a functional BH4 domain.

Lee et al. [23] have shown previously, by immunoprecipitation, that Nr-13 can associate with Bax in vertebrate cells, suggesting that it might inhibit Bax activity. In this study we took advantage of the interaction trap, a yeast two-hybrid system, to explore the interactions between Nr-13 and other members of the Bcl-2 family. In a first attempt we detected a strong intrinsic transcriptional activity of the LexA–Nr-13 fusion protein, before co-expression of any activation-domain fusion protein (results not shown). To overcome this difficulty we chose to use truncations of Nr-13. We generated three different truncations: fragment 1–52 (containing α-helices 1 and 2), fragment 1–63 (containing α-helices 1–3), and fragment 58–157 (containing α-helices 5 and 6). None of these truncations showed residual transcriptional activity when fused to LexA. Several Bcl-2 family members were
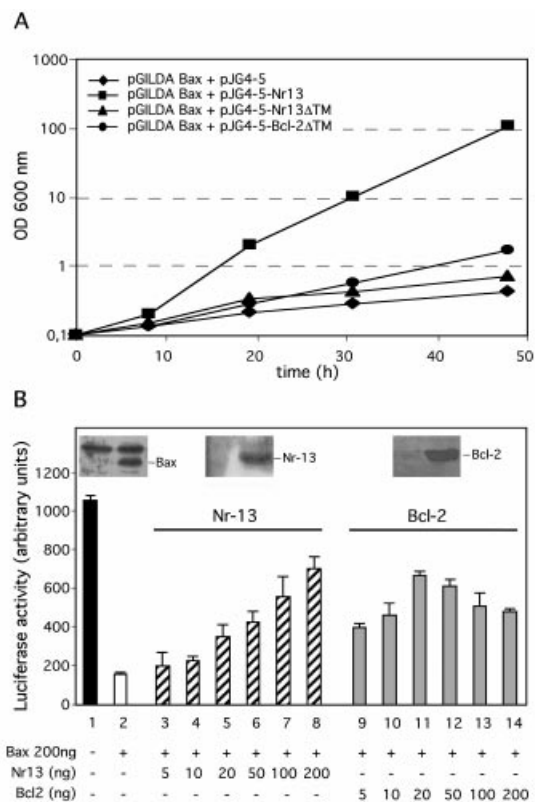
fused to the B42 transcription activation domain as prey. In all cases, the putative transmembrane domains were omitted to ensure proper nuclear localization of the fusion proteins. We were not able to detect interactions between any of the Nr-13 truncations and Bcl-2 or Bcl-xL. In contrast, truncation 58–157, which contains BH1 and BH2 but lacked the hydrophobic tail (TM domain), could efficiently form a complex with Bax and Bcl-xS while fragments 1–52 and 1–63 were unable to do so (Figure 2A). This strongly suggests that the region encompassing BH1 and BH2 contains the Bax and Bcl-xS interacting domain(s) of Nr-13. It also suggests that regions located outside this particular domain are unable to bind Bax and Bcl-xS, at least directly. It should be noted that the interaction of Nr-13 with Bax was seen only when Nr-13 was fused to LexA and Bax to B42, in the other permutation no interaction was observed. This is probably due to conformation of the fusion protein, which could hide domains which are indispensable for interaction. The same phenomenon has been reported previously with Bax plus Bcl-xL or A1/BFL-1 [6,37].

We then mapped the region of Bax responsible for the interaction with Nr-13 using the same two-hybrid system. Interac-
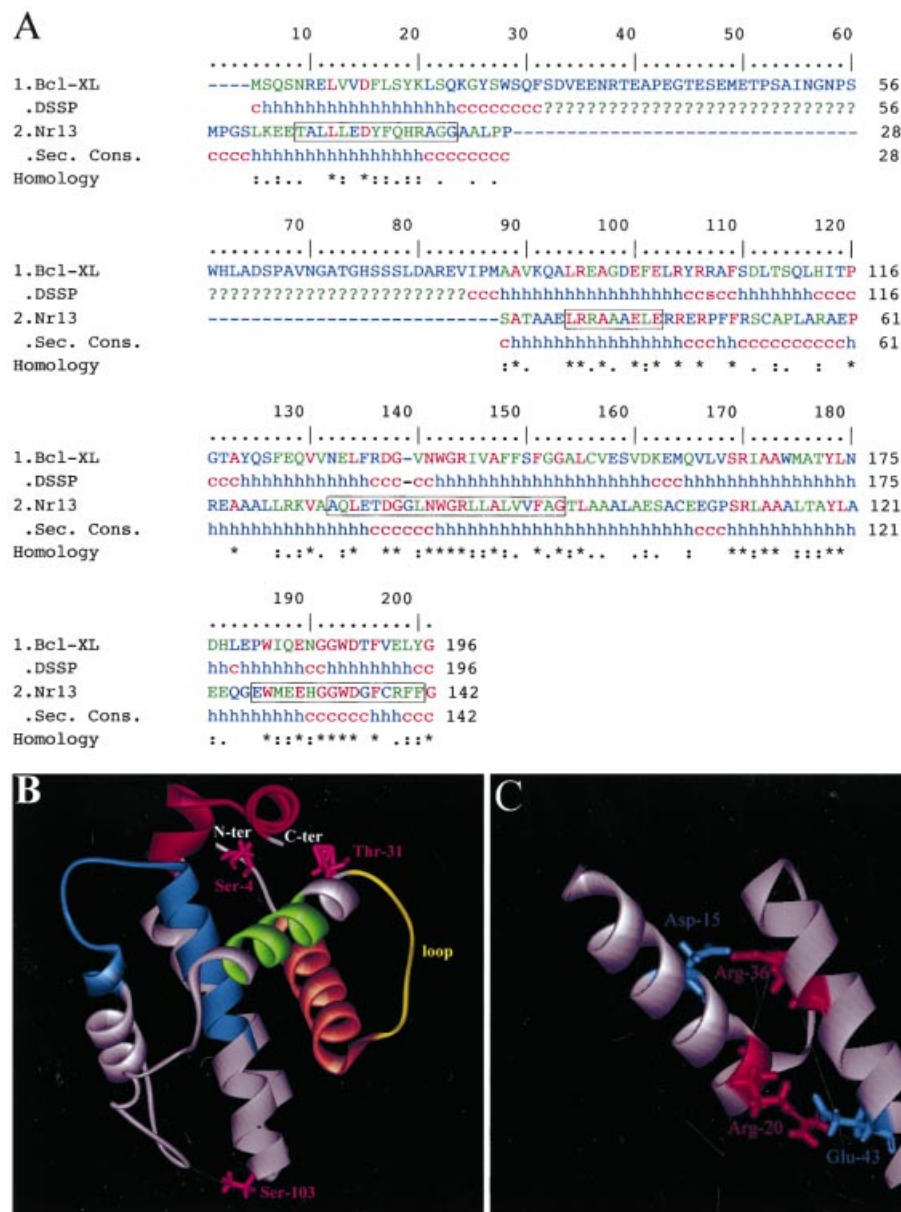
A
```
                  10        20        30        40        50        60
         .........|.........|.........|.........|.........|.........|
1.Bcl-XL    ----MSQSNRELVVDFLSYKLSQKGYSWSQFSDVEENRTEAPEGTESEMETPSAINGNPS  56
.DSSP          chhhhhhhhhhhhhhhhhhcccccccc????????????????????????????? 56
2.Nr13      MPGSLKEETALLLEDYFQHRAGGAALPP--------------------------------  28
.Sec. Cons.    cccchhhhhhhhhhhhhhhhhhcccccccc                                28
Homology        :.:.. *: *::.:: . . .

                  70        80        90       100       110       120
         .........|.........|.........|.........|.........|.........|
1.Bcl-XL    WHLADSPAVNGATGHSSSLDAREVIPMAAVKQALREAGDEFELRYRRAFSDLTSQLHITP 116
.DSSP       ?????????????????????????ccchhhhhhhhhhhhhhhhhhccscchhhhhhhcccc 116
2.Nr13      -------------------------SATAAELRRAAAELERRERPFFRSCAPLARAEP  61
.Sec. Cons.                          chhhhhhhhhhhhhhhhhhcccchhcccccccccccch  61
Homology                             :*.   **.*. *:* * *  *. .:. : *

                 130       140       150       160       170       180
         .........|.........|.........|.........|.........|.........|
1.Bcl-XL    GTAYQSFEQVVNELFRDG-VNWGRIVAFFSFGGALCVESVDKEMQVLVSRIAAWMATYLN 175
.DSSP       ccchhhhhhhhhhhccc-cchhhhhhhhhhhhhhhhhhhccchhhhhhhhhhhhhhhhh 175
2.Nr13      REAAALLRKVAAQLETDGGLNWGRLLALVVFAGTLAAALAESACEEGPSRLAAAALTAYLA 121
.Sec. Cons. hhhhhhhhhhhhhhcccccchhhhhhhhhhhhhhhhhhhhccchhhhhhhhhhhhhhhh 121
Homology     *   :.:*. :* ** :****::*:. *.*:*.. .:. : **:** :::**

                 190       200
         .........|.........|.|.
1.Bcl-XL    DHLEPWIQENGGWDTFVELYG 196
.DSSP       hhchhhhhhcchhhhhhhhcc 196
2.Nr13      EEQGEWMEEHGGWDGFCRFFG 142
.Sec. Cons. hhhhhhhhhcccccchhhccc 142
Homology    :.   *::*:**** * .::*
```

Figure 4   3D structure of Nr-13 as modelled from Bcl-xL structure

(**A**) Alignment between Bcl-xL and Nr-13. The human Bcl-xL and chicken Nr-13 sequences were aligned with the CLUSTALW 1.8 program (default parameters of the NPS@ server http://npsa-pbil.ibcp.fr). The consensus of secondary structure prediction obtained by DSC [51], PHD [52] and SOPMA [53] is given in the 'Sec. Cons.' lane. The observed secondary structure of BcL-xL was deduced from 1MAZ structure by using the DSSP program [54]. h, helix; c, coil and ?, unresolved structure. Boxes indicate the boundaries of BH4 [8–23], BH3 [35–43], BH2 [126–141], and BH1 [73–94] onto the Nr-13 protein. (**B**) Structure obtained using the XPLOR software. The typical organization of Bcl-2-like proteins with 7 α-helices is shown. BH domains are shown in different colours (orange, BH4; green, BH3; blue, BH1 and red, BH2). The short loop [24–30] is shown in yellow. A 3D representation of this structure is shown at http://www.BiochemJ.org/bj/368/bj3680213add.htm. (**C**) Residues involved in ionic bonds between BH4 and BH3 regions of Nr-13 are Asp15–Arg36 and Arg20–Glu43. Aspartate and glutamate are in blue and arginines are in red.

tions between region 58–157 of Nr-13 (containing BH1 and BH2) and various Bax truncations (shown in Figure 2B) are listed in Figure 2(C). Taken together, these results show that all BH3-containing Bax truncations interact with Nr-13. In contrast, Bax mutants 1–63 and 71–144, lacking BH3, are unable to bind to Nr-13. Although Bax BH3 domain alone cannot bind to Nr-13, probably reflecting the necessity of flanking sequences for correct folding of the fusion protein (construct 54–77, Figure 2C), these results show that BH3 is necessary for interaction with Nr-13. Moreover, on the basis of Bcl-xL 3D structure, indicating that

BH1 and BH2 form an hydrophobic binding site for BH3 domains of apoptosis inductors, it is likely that Bax also interacts with Nr-13 through its BH3 domain. These observations confirm that Nr-13 can dimerize with Bax, and potentially behaves as an anti-Bax protein. To directly assess this point we investigated the functional significance of this interaction in yeast. As previously reported [32,33], Bax induces death in the yeast *Saccharomyces cerevisiae* (Figure 3A) and this effect is dependent on the TM region. By studying growth of transfected EGY48 yeast for 2 days, we showed that co-expression of Nr-13 can very efficiently
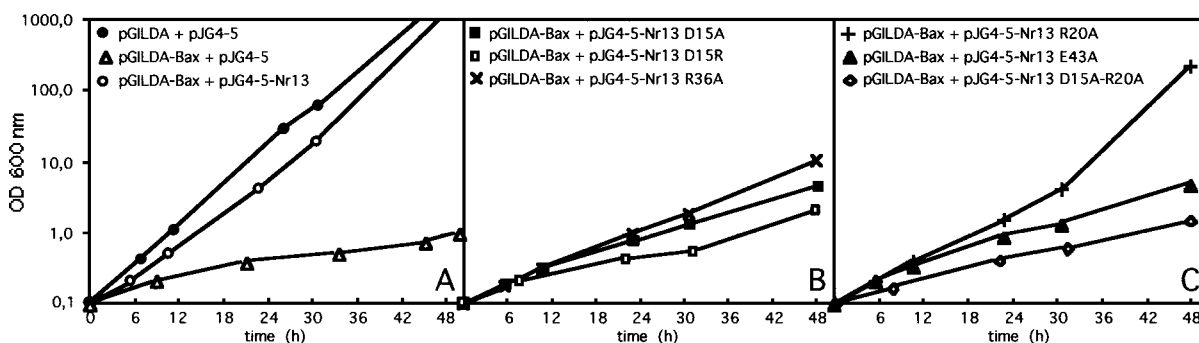
Figure 5   Electrostatic interactions between BH4 and BH3 are essential for Nr-13 anti-death activity in yeast

Growth curves of EGY48 yeast strains expressing Bax and Nr-13. (**A**) Effect of empty vectors, Bax alone, or Bax co-expressed with wt Nr-13. (**B**) Disruption of the most external bond of Nr-13. (**C**) Disruption of the internal ionic bond (R20A and E43A curves) or both bonds (D15A–R20A).

counteract Bax cytotoxicity in yeast (Figure 3A). A similar effect has been described for Bcl-xL, Bcl-2, Mcl-1, A1/BFL-1 and Nrh [6,33,36,38] while the necessity of the TM segment in this mechanism is still controversial [38,39]. In our study, absence of the Nr-13 putative TM segment completely abolished its ability to counteract Bax-induced lethality, as for Bcl-2 ΔTM (Figure 3A).

In order to confirm these results in mammalian cells we used a transient-transfection system in Rat-1 fibroblasts as described previously [40,41]. Apoptotic regulatory genes under the control of a CMV promoter were cotransfected with the luciferase reporter gene into Rat-1 cells. Luciferase activity assays were performed 18 h after lipofection and expression of Bax, Bcl-2 and Nr-13 proteins was simultaneously checked by Western blot. Co-transfection of Bax with the luciferase reporter gene resulted in a 6-fold decrease in luciferase activity. Co-expression of Bcl-2 partially restored luciferase activity before reaching a plateau, while co-expression of Nr-13 restored luciferase activity in a dose-dependent manner (Figure 3B). Decrease of luciferase activity in this system has been shown previously to parallel the loss of viability [40].These results both in yeast and mammalian cells indicate that Nr-13 counteracts the pro-apoptotic activity of Bax.

Molecular modelling of Nr-13

The results presented so far suggest that the mode of action of Nr-13 is, at least in part, similar to other Bcl-2 family members (e.g. Bcl-xL, Bcl-2, A1/BFL-1). However, the poor homology between Nr-13 and other Bcl-2-related proteins, particularly in the N-terminal moiety, indicated that Nr-13 may exhibit distinct features. Nr-13 is one of the smallest anti-apoptotic members identified so far in the Bcl-2 family, especially because of the small size of the loop between BH4 and BH3 (Figure 1). We focused on the BH4 domain of Nr-13 and used computer-assisted molecular modelling to identify specific amino-acid residues potentially involved in the control of Nr-13 activity. A 3D structure of Nr-13 has been calculated using the structure of Bcl-xL, determined by crystallography and NMR, as a template [10]. Nr-13 showed the same organization as Bcl-xL with seven α-helices (Figure 4), two of them (α5 and α6) being critical for membrane insertion and pore formation [12].

The structure shown in Figure 4(B) is one of ten possible models for Nr-13. When superimposed at the level of α-carbons of all helices found in the protein, the ten 3D structures exhibited

a root-mean-square deviation (RMSD) of 0.42 Å (1 Å = 0.1 nm), indicating good convergence of the models (results not shown). The model shown in Figure 4(B) showed good geometry (93 % of residues located in the favourable region of the Ramachandran plot, low energy (−416 kcal/mol) and chemical features (RMSD of 0.94×10^{-2} Å and 2.6 ° for bonds and angles, respectively). These values were consistent with all ten models.

An interesting feature of Nr-13 is the position of three potential phosphorylation sites (S4, Y31, S103), two of them belonging to BH4/BH3 domains. These residues are located at the surface of the protein and are potentially accessible for kinases or phosphatases (Figure 4B). Recent evidence indicates that anti-apoptotic functions of Bcl-2 can be regulated by its phosphorylation and that multi-site phosphorylation of the Bcl-2 loop domain regulates cell death (review in [42]). It was reported recently that the induction of S70 phosphorylation could result in a loss of the binding ability of Bcl-2 with Bax which induces subsequent cell death [43]. By analogy, the three residues exposed at the surface of Nr-13 could be involved in the regulation of Nr-13 activity. In addition, the 3D structure points out two remarkable features of Nr-13: the very short loop in the vicinity of BH3 and BH4, suggesting an interaction between these two domains, which could be of functional significance.

Interaction between BH4 and BH3 is essential for Nr-13 activity

The model of the Nr-13 protein reveals that even if the connecting loop is very short (11 amino acids in Nr-13 instead of 69 in Bcl-xL) it is possible to locate BH4 and BH3 in the same orientation as in other Bcl-2 family members. It also suggests that electrostatic interactions are important to determine the position of BH4 with respect to BH3. Careful analysis of the Nr-13 model suggested the presence of two potential ionic bonds between BH4 and BH3 (D15–R36 and R20–E43, see Figure 4C) which may contribute to the stabilization of Nr-13 3D structure. To evaluate their functional significance, we decided to disrupt independently each of these ionic bonds by point mutations and to check for the anti-Bax activity of the corresponding Nr-13 mutants, both in yeasts and in Rat-1 cells.

First, the assay described previously in yeast was used to analyse the importance of these bonds. Compared to wt Nr-13 (Figure 5A), Figure 5(B) shows that disruption of the most external ionic bond by independent mutation of each of the residues (D15 and R36) results in nearly complete loss of activity of the protein in yeast, strongly suggesting that this ionic bond is
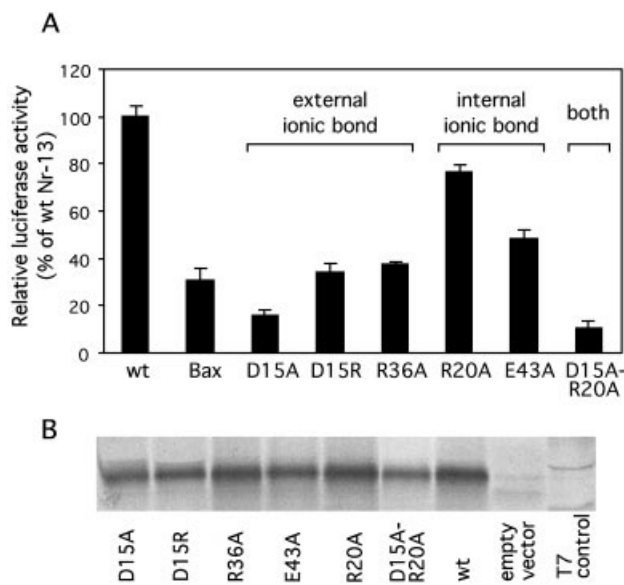
Figure 6   Electrostatic interactions between BH4 and BH3 are essential for Nr-13 anti-Bax activity in Rat-1 cells

(**A**) Bax induces loss of viability in Rat-1 fibroblasts which is inhibited by Nr-13 and at variable levels by Nr-13 mutants. Luciferase activity for each assay is presented as a percentage of an assay in which a reporter plus a Bax and a wt Nr-13 expression vector were transfected. Results are presented as means $\pm$ S.D. of three experiments. Destruction of ionic bonds between BH4 and BH3 by point mutations resulted in partial or total inactivation of the protein. (**B**) Translation and stability of proteins produced in Rat-1 cells were checked by *in vitro* coupled transcription/translation from the same vectors used for transfection in (**A**).

essential for Nr-13 activity. Mutation of E43, involved in the most internal bond, gives a similar result while the R20A mutation results in a less drastic phenotype. Altogether, these data are in accordance with the lower structural constraints exerted on the most internal bond as compared with the external bond. Disruption of both ionic bonds (D15A–R20A) results in completely inactive protein (Figure 5C). Production of wt and all the mutant Nr-13 fusion proteins in yeast was checked by SDS/PAGE using an anti-B42 polyclonal antibody (results not shown).

To confirm these results, we expressed the different mutated Nr-13 proteins in Rat-1 cells under the CMV promoter. Figure 6(A) shows that mutations D15A, D15R or R36A (all supposed to suppress the external ionic bond) again resulted in complete inhibition of the anti-apoptotic function of the protein. The two other mutations, R20A and E43A (targeting the internal ionic bond), resulted in partial or total inactivation respectively, as shown in yeast cells. In addition, the double mutant D15A–R20A, in which the two ionic bonds are disrupted, was again totally inactive. Figure 6(B) shows that all mutant proteins expressed in Rat-1 cells had a comparable expression level by coupled *in vitro* transcription–translation. However, a trivial explanation of the results could be that these mutations merely destabilize α-helices (BH4 or BH3), leading to incorrect folding of the protein.

To address this point, we synthesized two oligopeptides corresponding to amino acids 1–21 of Nr-13 and the D15A mutant. Both exhibited high helical content as checked by CD, even in the absence of 2,2,2-trifluoroethanol or SDS (results not shown). These data demonstrated the α-helical conformation of the BH4 mutant D15A. Thus, the effect of this mutation is not due to the destabilization of the helical structure of BH4.
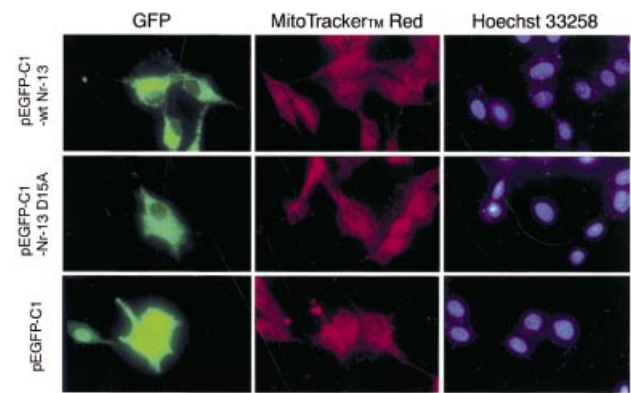

Figure 7   Subcellular localization of wild-type and mutant Nr-13 proteins in transient transfectants

QM7 cells that transiently express EGFP, wild-type or mutant EGFP-Nr-13 were observed by fluorescence microscopy. Mitochondria were visualized with MitoTracker™ Red and nuclei with Hoechst 33258. Upper series, cells expressing wt Nr-13; middle series, cells expressing D15A-R20A Nr-13; lower series, cells transfected with empty pEGFP-C1 vector. Same observations were performed in COS-7 cells (not shown).

Therefore, the effect of the point mutations described above is likely due to ionic-bond disruption between BH4 and BH3.

Mutation of the ionic bonds does not alter subcellular localization

Bcl-2-related proteins are associated with the outer mitochondrial membrane, where they may monitor the interaction of cytochrome *c* with the inner mitochondrial membrane by imperfectly elucidated mechanisms. Whereas Bcl-xL is permanently associated with mitochondria, Bax, which is normally sequestered in the cytosol, is directed towards the outer mitochondrial membrane following an apoptotic stimulus. To check if mutation of residues involved in ionic bonds could affect Nr-13 localization, we generated EGFP-Nr-13 expression vectors and transfected them into both COS-7 and QM7 cells to explore Nr-13 localization by immunocytochemistry. As shown in Figure 7, EGFP protein localization is both nuclear and cytoplasmic, while fusion EGFP-Nr-13 protein is cytoplasmic in QM7 cells. The same result was obtained using COS-7 cells (results not shown). Mitotracker™ labelling shows that Nr-13 partly co-localizes with mitochondria. All mutants show a subcellular distribution identical to the wild-type protein, especially the D15A–R20A double mutant which is totally devoid of anti-Bax activity. Thus, the lack of activity shown for Nr-13 proteins harbouring these mutations is not due to Nr-13-impaired subcellular localization.

DISCUSSION

In the present study we have tested the possibility that Nr-13 may contain a BH4 domain and studied its mechanism of action. On the basis of its homology with some Bcl-2 family members (Bcl-2, Bcl-xL, Bcl-w, A1/BFL-1, for example) in the region corresponding to the binding site for BH3-containing apoptosis inducers (α-helices 5–7), we forward the hypothesis that Nr-13 could dimerize with Bax. Lee et al. [23] had shown previously, by immunoprecipitation in the avian cell line DT40, that Nr-13 could co-precipitate with Bax. Here we have confirmed these results in yeast, using a yeast two-hybrid system. Our results show that the BH1 and BH2 regions are sufficient for this interaction. In contrast, BH4 and BH3 do not seem to interact

with Bax. These results, in agreement with previous studies on Bcl-xL and Bcl-2 [15,33], suggest by analogy that, in Nr-13 the hydrophobic cleft formed by BH1 and BH2 binds to the BH3 region of Bax. They also correlate with the recent demonstration of the high-affinity binding of a Bax BH3 peptide to Nr-13 as monitored by the intrinsic tryptophan fluorescence [24].

It was important, therefore, to evaluate the functional significance the Nr-13–Bax interaction. We have shown that Nr-13 was able to inhibit efficiently Bax-dependent cell death both in yeast and in vertebrate cells (Figure 3).

Several groups have reported previously that Bax induces growth arrest in the yeast *S. cerevisiæ* [32,33]. This no-growth phenotype was demonstrated to be caused by cell death [39]. In turn, whether or not this type of cell death was true apoptosis remained a key question. The ensuing studies gave equivocal results but favour an apoptotic-like mechanism [44], including cytochrome *c* release [45]. Here we show that Bax-induced growth-arrest in yeast can be very efficiently counteracted by Nr-13 (Figure 3A). Similar anti-Bax effects have been described for Bcl-xL, Bcl-2, Mcl-1 and A1/BFL-1 [6,33,38]. In the same way, a functional analysis has been carried out in Rat-1 cells. It clearly demonstrated that Nr-13 had a dose-dependent ability to counteract Bax effect in mammalian Rat-1 cells (Figure 3B). This is in agreement with similar studies on Bcl-2 using this experimental model [40,46] and clearly classifies Nr-13 among Bax antagonists.

To identify more precisely the amino acids residues critical for Nr-13 activity, we have generated a 3D model of Nr-13 by molecular modelling from Bcl-xL structure, as determined by crystallography and NMR studies. Ten structures of Nr-13 were generated, all exhibiting very similar features. Indeed, all the structures shared homogeneous and satisfactory properties (good geometry, low energy and low RMSD). This modelling approach has demonstrated the geometric possibility of connecting BH3 and the N-terminal part of Nr-13 even with the shortest peptide (11 residues instead of 69 in Bcl-xL) known in this family (Figure 4B). The CD spectrum demonstrated the helical organization of this isolated N-terminal region. A careful analysis of the Nr-13 models has revealed the presence of two potential ionic bonds between BH4 and BH3. Indeed, selected disruption by point mutation of each of these bonds leads to a complete (D15A, D15R, R36A or E43A) or partial (R20A) inactivation of Nr-13, both in yeast and mammalian cells. Since these mutations do not seem to alter the α-helix secondary structure, as checked by CD, it is likely that these ionic bonds are essential for Nr-13 activity.

The results reported here are the first experimental demonstration of the existence of BH4 in Nr-13 and the functional role of electrostatic interactions between charged residues in the BH4 and BH3 domains of Nr-13. Interestingly, one of them (D15-R36) has been conserved in a number of Bcl-2 family members such as Bcl-xL, Bcl-w and Mcl-1, but not in all of them, since it was not found in Bcl-2, Boo or CED-9 (Figure 8). This latter observation indicates that different regulatory mechanisms might exist, depending on the subfamily of Bcl-2 proteins. Indeed this diversity between BH4 regions could allow a fine regulation by these proteins, for example, through the binding of specific regulatory partners.

The results presented herein allow us to speculate that two conformations might exist for Nr-13, differing by the position of BH4 relative to the rest of the protein. Indeed, the interactions between BH4 and BH3 may stabilize the active conformation; a disruption of these interactions (e.g. change in ionic strength) would therefore lead to a displacement of BH4 and to the inactivation of Nr-13. At the same time, the inactive form may loose its capacity to bind to specific partners (VDAC, Raf-1, Apaf-1, calcineurin, etc.). Finally, on the basis of the structural

A

```
NR13   CHICK    5 LKEETALLLEDYFQHRAGGAALPPSAT   31
BCLXL  CHICK    1 MSSSNRELVIDFVSYKLSQRGHCWSEL   27
BCLW   HUMAN    6 SAPDTRALVADFVGYKLRQKGYVCGAG   32

BCL2   HUMAN    7 TGYDNREIVMKYIHYKLSQRGYEWDAG   33
CED9   WORM    18 NTFRRRTMATSEMREFLSTKDAEPNNF   44
BOO    MOUSE    8 LHERTRRLLSDYIFFCAREPDTPEPPP   34
Homology            :  .  .
```

B

```
NR13   CHICK   32 AAELRRAAAELERRERPFFRSCAPLARAEPREAAALLRKVAAQLEAEG   79
BCLXL  CHICK   83 RQALRDAGDEFELRYRRAFSDLTSQLHITPGTAYQSFEQVVNELFHDG  130
BCLW   HUMAN   43 HQAMRAAGDEFETRFRRTFSDLAAQLHVTPGSAQQRFTQVSDELFQGG   90

BCL2   HUMAN   94 HLTLRQAGDDFSRRYRRDFAEMSSQLHLTPFTARGRFATVVEELFRDG  141
CED9   WORM   113 HEMMRSLGTIFEKRHMEMFENFSEQLLAVPKISFSLYQEVVQTVGNSS  160
BOO    MOUSE   35 TSVEAALLRSVTRQIQQEHQEFFSSFCESRGNRLELVKQMADKLLSKD   82
Homology           .  :  .  ..           :   :  .
```

Figure 8   Comparison of N-terminal regions suggests existence of sub-families of anti-apoptotic proteins

Multiple sequence alignment of BH4 (**A**) and BH3 (**B**) regions of Bcl-2 family members. Conserved residues appear in bold. Bcl-xL and Bcl-w both have an aspartate (D) in BH4 and an arginine (R) in BH3 at similar positions compared to Nr-13, strongly suggesting that BH4 and BH3 interact also through an ionic bond in these proteins. In contrast, no such conservation was observed in Bcl-2, Boo or Ced-9, indicating that this ionic bond is absent in this subgroup of anti-apoptotic proteins.

homology with bacterial colicins, these two putative conformations may correspond to the open or closed states of an ionic channel [10,47]. The targeted disruption of interactions between BH4 and BH3 by molecules such as synthetic peptides could be a valuable therapeutic strategy for diseases caused by apoptosis deregulation.

REFERENCES

1   Evan, G. and Littlewood, T. (1998) A matter of life and death. Science (Washington, D.C.) **281**, 1317–1322

2   Adams, J. M. and Cory, S. (1998) The Bcl-2 protein family: arbiters of cell survival. Science (Washington, D.C.) **281**, 1322–1326

3   Wei, M. C., Zong, W. X., Cheng, E. H., Lindsten, T., Panoutsakopoulou, V., Ross, A. J., Roth, K. A., MacGregor, G. R., Thompson, C. B. and Korsmeyer, S. J. (2001) Proapoptotic BAX and BAK: a requisite gateway to mitochondrial dysfunction and death. Science (Washington, D.C.) **292**, 727–730

4   Oltvai, Z. N., Milliman, C. L. and Korsmeyer, S. J. (1993) Bcl-2 heterodimerizes in vivo with a conserved homolog, Bax, that accelerates programmed cell death. Cell (Cambridge, Mass.) **74**, 609–619

5   Minn, A., Kettlun, C. S., Liang, H., Kelekar, A., Vander Heiden, M. G., Chang, B. S., Fesik, S. W., Fill, M. and Thompson, C. B. (1999) Bcl-xL regulates apoptosis by heterodimerization-dependent and -independent mechanisms. EMBO J. **18**, 632–643

6   Zhang, H., Cowan-Jacob, S. W., Simonen, M., Greenhalf, W., Heim, J. and Meyhack, B. (2000) Structural basis of BFL-1 for its interaction with Bax and its anti-apoptotic action in mammalian and yeast cells. J. Biol. Chem. **275**, 11092–11099

7   Nechushtan, A., Smith, C. L., Lamensdorf, I., Yoon, S. H. and Youle, R. J. (2001) Bax and Bak coalesce into novel mitochondria-associated clusters during apoptosis. J. Cell Biol. **153**, 1265–1276

8   Adams, J. M. and Cory, S. (2001) Life-or-death decisions by the Bcl-2 protein family. Trends Biochem. Sci. **26**, 61–66

9 Gross, A., McDonnell, J. M. and Korsmeyer, S. J. (1999) BCL-2 family members and the mitochondria in apoptosis. Genes Dev. **13**, 1899–1911

10 Muchmore, S. W., Sattler, M., Liang, H., Meadows, R. P., Harlan, J. E., Yoon, H. S., Nettesheim, D., Chang, B. S., Thompson, C. B., Wong, S. L. et al. (1996) X-ray and NMR structure of human Bcl-xL, an inhibitor of programmed cell death. Nature (London) **381**, 335–341

11 Schendel, S. L., Xie, Z., Montal, M. O., Matsuyama, S., Montal, M. and Reed, J. C. (1997) Channel formation by antiapoptotic protein Bcl-2. Proc. Natl. Acad. Sci. U.S.A. **94**, 5113–5118

12 Reed, J. C. (1997) Double identity for proteins of the Bcl-2 family. Nature (London) **387**, 773–776

13 Suzuki, M., Youle, R. J. and Tjandra, N. (2000) Structure of Bax : coregulation of dimer formation and intracellular localization. Cell (Cambridge, Mass.) **103**, 645–654

14 McDonnell, J. M., Fushman, D., Milliman, C. L., Korsmeyer, S. J. and Cowburn, D. (1999) Solution structure of the proapoptotic molecule BID : a structural basis for apoptotic agonists and antagonists. Cell (Cambridge, Mass.) **96**, 625–634

15 Huang, D. C., Adams, J. M. and Cory, S. (1998) The conserved N-terminal domain of Bcl-2 homologues is essential for inhibition of apoptosis and interaction with CED-4. EMBO J. **17**, 1029–1039

16 Lee, L. C., Hunter, J. J., Mujeeb, A., Turck, C. and Parslow, T. G. (1996) Evidence for α-helical conformation of an essential N-terminal region in the human Bcl-2 protein. J. Biol. Chem. **271**, 23284–23288

17 Hirotani, M., Zhang, Y., Fujita, N., Naito, M. and Tsuruo, T. (1999) NH2-terminal BH4 domain of Bcl-2 is functional for heterodimerization with Bax and inhibition of apoptosis. J. Biol. Chem. **274**, 20415–20420

18 Shimizu, S., Konishi, A., Kodama, T. and Tsujimoto, Y. (2000) BH4 domain of antiapoptotic Bcl-2 family members closes voltage-dependent anion channel and inhibits apoptotic mitochondrial changes and cell death. Proc. Natl. Acad. Sci. U.S.A. **97**, 3100–3105

19 Shibasaki, F., Kondo, E., Akagi, T. and McKeon, F. (1997) Suppression of signalling through transcription factor NF-AT by interactions between calcineurin and Bcl-2. Nature (London) **386**, 728–731

20 Gillet, G., Michel, D., Crisanti, P., Herault, Y., Pessac, B., Calothy, G., Brun, G. and Volovitch, M. (1993) Serum factors and v-*src* control two complementary mitogenic pathways in quail neuroretinal cells in culture. Oncogene **8**, 565–574

21 Gillet, G., Guerin, M., Trembleau, A. and Brun, G. (1995) A Bcl-2-related gene is activated in avian cells transformed by the Rous sarcoma virus. EMBO J. **14**, 1372–1381

22 Mangeney, M., Schmitt, J. R., Leverrier, Y., Thomas, J., Marvel, J., Brun, G. and Gillet, G. (1996) The product of the v-src-inducible gene *nr-13* is a potent anti-apoptotic factor. Oncogene **13**, 1441–1446

23 Lee, R. M., Gillet, G., Burnside, J., Thomas, S. J. and Neiman, P. (1999) Role of Nr13 in regulation of programmed cell death in the bursa of Fabricius. Genes Dev. **13**, 718–728

24 Moradi-Améli, M., Lorca, T., Ficheux, D., Di Pietro, A. and Gillet, G. (2002) Interaction between the antiapoptotic protein Nr-13 and cytochrome c. Antagonistic effect of the BH3 domain of Bax. Biochemistry **41**, 8540–8550

25 Thompson, J. D., Higgins, D. G. and Gibson, T. J. (1994) CLUSTAL W : improving the sensitivity of progressive multiple sequence alignment through sequence weighting, position-specific gap penalties and weight matrix choice. Nucleic Acids Res. **22**, 4673–4680

26 Combet, C., Jambon, M., Deléage, G. and Geourjon, C. (2002) Geno3D : automatic comparative molecular modelling of protein. Bioinformatics **18**, 213–214

27 Brunger, A. T. (1982) X-PLOR : a system for X-ray crystallography and NMR. Version 3.1 manual, Yale University Press, New Haven CT

28 Laskowski, R. A., MacArthur, M. W., Moss, D. S. and Thornton, J. M. (1993) PROCHECK : a program to check the stereochemical quality of protein structures. J. Appl. Cryst. **26**, 283–291

29 Finley, R. L., Jr and Brent, R. (1994) Interaction mating reveals binary and ternary connections between *Drosophila* cell cycle regulators. Proc. Natl. Acad. Sci. U.S.A. **91**, 12980–12984

30 Golemis, E. A. and Brent R. (1997) In The yeast two-hybrid system (Bartel, P. L. and Fields, S., eds.), pp. 43–72. Oxford University Press, New York–Oxford

31 Golemis, E. A., Serebriiskii, I., Finley, R. L., Jr, Kolonin, M. G., Gyuris, J. and Brent, R. (1999). In Current Protocols in Molecular Biology, vol. 4 (Ausubel, F. M., Brent, R., Kingston, R. E., Moore, D. D., Smith, J. A. and Struhl, K., eds.), pp. 20.1.1–20.1.40, John Wyley & Sons, Inc.

32 Sato, T., Hanada, M., Bodrug, S., Irie, S., Iwama, N., Boise, L. H., Thompson, C. B., Golemis, E., Fong, L., Whang, H.-G. and Reed, J. C. (1994) Interactions among members of the Bcl-2 protein family analyzed with a yeast two-hybrid system. Proc. Natl. Acad. Sci. U.S.A. **91**, 9238–9242

33 Hanada, M., Aimé-Sempé, C., Sato, T. and Reed, J. C. (1995) Structure–function analysis of Bcl-2 protein. Identification of conserved domains important for homodimerization with Bcl-2 and heterodimerization with Bax. J. Biol. Chem. **270**, 11962–11969

34 Gietz, R. D., Schiestl, R. H., Willems, A. R. and Woods, R. A. (1995) Studies on the transformation of intact yeast cells by the LiAc/SS-DNA/PEG procedure. Yeast **11**, 355–360

35 Chen, Y. H., Yang, J. T. and Chau, K. H. (1974) Determination of the helix and beta form of proteins in aqueous solution by circular dichroism. Biochemistry **13**, 3350–3359

36 Aouacheria, A., Arnaud, E., Venet, S., Lalle, P., Gouy, M., Rigal, D. and Gillet, G. (2001) Nrh, a human homologue of Nr-13 associates with Bcl-Xs and is an inhibitor of apoptosis. Oncogene **20**, 5846–5855

37 Simonen, M., Keller, H. and Heim, J. (1997) The BH3 domain of Bax is sufficient for interaction of Bax with itself and with other family members and it is required for induction of apoptosis. Eur. J. Biochem. **249**, 85–91

38 Tao, W., Kurschner, C. and Morgan, J. I. (1997) Modulation of cell death in yeast by the Bcl-2 family of proteins. J. Biol. Chem. **272**, 15547–15552

39 Greenhalf, W., Stephan, C. and Chaudhuri, B. (1996) Role of mitochondria and C-terminal membrane anchor of Bcl-2 in Bax induced growth arrest and mortality in *Saccharomyces cerevisiae*. FEBS Lett. **380**, 169–175

40 Wang, K., Yin, X. M., Chao, D. T., Milliman, C. L. and Korsmeyer, S. J. (1996) BID : a novel BH3 domain-only death agonist. Genes Dev. **10**, 2859–2869

41 Wang, K., Gross, A., Waksman, G. and Korsmeyer, S. J. (1998) Mutagenesis of the BH3 domain of BAX identifies residues critical for dimerization and killing. Mol. Cell. Biol. **18**, 6083–6089

42 Blagosklonny, M. V. (2001) Unwinding the loop of Bcl-2 phosphorylation. Leukemia **15**, 869–874

43 Shitashige, M., Toi, M., Yano, T., Shibata, M., Matsuo, Y. and Shibasaki, F. (2001) Dissociation of bax from a bcl-2/bax heterodimer triggered by phosphorylation of serine 70 of bcl-2. J. Biochem. **130**, 741–748

44 Ligr, M., Madeo, F., Fröhlich, E., Hilt, W., Fröhlich, K.-U. and Wolf, D. H. (1998) Mammalian Bax triggers apoptotic changes in yeast. FEBS Lett. **438**, 61–65

45 Priault, M., Camougrand, N., Chaudhuri, B. and Manon, S. (1999) Role of the C-terminal domain of Bax and Bcl-XL in their localisation and function in yeast cells. FEBS Lett. **443**, 225–228

46 Nechushtan, A., Smith, C., Hsu, Y. and Youle, R. (1999) Conformation of the Bax C-terminus regulates subcellular location and cell death. EMBO J. **18**, 2330–2341

47 Zakharov, S. D., Lindeberg, M., Griko, Y., Salamon, Z., Tollin, G., Prendergast, F. G. and Cramer, W. A. (1998) Membrane-bound state of the colicin E1 channel domain as an extended two-dimensional helical array. Proc. Natl. Acad. Sci. U.S.A. **95**, 4282–4287

48 Lee, R., Chen, J., Matthews, C. P., McDougall, J. K. and Neiman, P. E. (2001) Characterisation of *NR13*-related human cell death regulator, *Bool/Diva*, in normal and cancer tissues. Biochim. Biophys. Acta **1520**, 187–194.

49 Zhang, H., Holzgreve, W. and De Geyter, C. (2001) Bcl2-L-10, a novel anti-apoptotic member of the Bcl-2 family, blocks apoptosis in the mitochondria death pathway but not in the death receptor pathway. Hum. Mol. Genet. **10**, 2329–2339

50 Ke, N., Godzik, A. and Reed, J. C. (2001) Bcl-B, a novel Bcl-2 family member that differentially binds and regulates Bax and Bak. J. Biol. Chem. **276**, 12481–12484

51 King, R. D. and Sternberg, M. J. (1996) Identification and application of the concepts important for accurate and reliable protein secondary structure prediction. Protein Sci. **5**, 2298–2310

52 Rost, B. and Sander, C. (1993) Prediction of protein secondary structure at better than 70 % accuracy. J. Mol. Biol. **232**, 584–599

53 Geourjon, C. and Deléage, G. (1995) SOPMA : significant improvements in protein secondary structure prediction by consensus prediction from multiple alignments. Comput. Appl. Biosci. **11**, 681–684

54 Kabsch, W. and Sander, C. (1983) How good are predictions of protein secondary structure ? FEBS Lett. **155**, 179–182